Electronic Supplementary Material (ESI) for Environmental Science: Processes & Impacts.

Supplementary Information

An uneven distribution of strontium in the coccolithophore *Scyphosphaera apsteinii* revealed by 3D X-ray fluorescence

Jessica M. Walker[1], Hallam J. M. Greene[1,2], Y. Moazzam[1], P. D. Quinn[1], J. E. Parker[1], G. Langer[3]

[1] Diamond Light Source, Harwell Science and Innovation Campus, Didcot, OX11 0DE

[2] Department of Chemistry, University of Sheffield, Dainton Building, Brook Hill, Sheffield S3 7HF

[3] Institute of Environmental Science and Technology, Barcelona, Spain

Methods

At Diamond Light Source, clonal cultures of *Scyphosphaera apsteinii* (RCC1456) were grown at 19 °C in a 12h:12h, light:dark cycle in f/2 media at a light intensity of approximately 150-200 µmol m^{-2} s^{-1}. f/2 media was prepared using filtered (Nalgene Rapid-Flow sterile filter units with PES membranes, 0.2 µm pore size), aged (>3 months) surface seawater gathered from the Bristol Channel near Mumbles Head, Gower (51.560675° N, -3.979134° W), supplemented with f/2 nutrients, and further enriched with 3 nM nickel chloride and 5 nM selenous acid. *S. apsteinii* (RCC1456) cultured at Marine Biological Association (MBA), Plymouth was grown in aged (3 months), sterile-filtered (Stericup-GP Sterile Vacuum Filtration System, 0.22 µm pore size, polyethersulphone membrane; Merck, Gillingham, UK) natural surface seawater sampled in the English Channel off Plymouth, UK (station E1: 50°2.00′N, 4°22.00′W), enriched with 100 µM nitrate, 6.25 µM phosphate, 5nM selenous acid, 3.14 nM nickel chloride, and trace metals and vitamins as in f/2 medium.[1] Cultures were grown under a 16h:8h, light:dark cycle at a light intensity of 50–70 µmol m^{-2} s^{-1} in temperature-controlled culture rooms at 18 °C. Cells were grown in dilute batch cultures, ensuring a quasi-constant seawater carbonate system over the course of the experiment.[2]

S. apsteinii (RCC1456) was obtained from the Roscoff Culture Collection (http://www.roscoff-culture-collection.org). Cultures at approx. 10,000 cells per mL were centrifuged at 500 rpm for 10 minutes to pellet the coccoliths (RCF 58 ×g) before washing with milliQ water raised to pH 9.5.

For higher [Sr] cultures: Sr-free artificial seawater was prepared (as detailed in **Table S1**) using ultrapure water. The seawater was further enriched with f/2 nutrients and supplemental additions, and filter sterilised as previously detailed. To this was added 1 mL natural seawater (Gower) per L artificial seawater. The Sr concentration was adjusted by the addition of 1 M aqueous solution of $SrCl_2$. 30 mL portions of artificial f/2 media at different Sr concentrations were each inoculated with 1 mL samples from a stock culture of *S. apsteinii* (ca 10,000 cells per mL). After 15 days, three 10 mL aliquots from each culture were transferred into 300 mL portions of the same growing medium, initiating large-scale cultures at each Sr concentration in triplicate. After a further 12 days, cultures (estimated density 1000 cells cm^{-3}) were pelleted by two rounds of centrifugation (RCF ~4000× g). These were transferred to 1.5 mL microcentrifuge tubes using small quantities of ultrapure water, raised to pH 9.5 by the addition of NH_4OH(aq). These were centrifuged (RCF 1700× g) for 10 minutes and the supernatant removed. Coccoliths were resuspended in 3 × 1 mL of the same pH-adjusted water, centrifuging in the same manner between washes. Following this treatment, coccoliths were suspended in ethanol and small samples drop cast onto silicon nitride windows.

For 3D XRF, coccoliths were pin-mounted: A portion of the coccoliths were suspended in ethanol and drop cast onto a glass cover slip. Selecting complete, isolated coccoliths with normal morphology under a light microscope, coccoliths were mounted on stainless steel pins (Austerlitz Insect Pins size 000) with epoxy resin using a micromanipulator (MicroSupport Axis Pro).

For 2D XRF coccoliths were mounted on silicon nitride windows: Rinsed coccoliths were suspended in ethanol and drop cast onto silicon nitride windows (500 nm membrane thickness).

XRF imaging and tomography: XRF experiments were performed at the I14 hard X-ray nanoprobe beamline at Diamond Light Source.[3] A beam energy of 18 keV was used in all XRF, XRF tomography, and imaging experiments with a nominal beam size of 50 nm. For 3D tomography, a field of view of 15 x 20 microns was used to accommodate jitter and drift during the scans. A count time of 0.02 s per point and a 60 nm step size were used for each map resulting in a collection time of 30 mins per map. 91 maps were collected at intervals of 2°. This resulted in a scan time of 45.5 hours for a 3D volume. Samples were mounted on insect pins (3D imaging) or on silicon nitride windows (2D imaging). In 2D, 4 specimens were imaged, with one different specimen imaged in 3D. Elemental mapping was achieved by summing the counts the fluorescent Kα X-rays of Ca and Sr within a 200 eV window. Differential phase contrast imaging was collected simultaneously for all measurements.[4] XRF maps are individually normalised from 0-1, the maximum counts per pixel are given in **Table S1**.

Data analysis and processing of the tomography was achieved using a series of custom scripts for alignment (centre-of mass)[5] and reconstruction.[6] Volume renderings and animations were created using the Avizo software package. Data processing and measurements, including image rotation and numerical determinations of Ca and Sr counts, were conducted using DAWN.[7] Image creation was performed using ImageJ.[8] Images showing Sr counts divided by Ca counts in each pixel were achieved after first thresholding the Ca map to remove background counts not associated with the coccolith. Following the tilt series, the sample was rotated to a side-on view where an XRF scan at a higher count time of 0.75 s and Sr K-edge XANES map of a transect was performed. For the Sr k-edge XANES, the area was mapped at 152 energies between 16.0 and 16.3 keV, and reconstructed using in-house custom scripts, before analysis using the Mantis software package.[9]

XANES standards: Standards were synthesized in house using a calcite synthesis was adapted from the work of Littlewood et al. (2017)[10] and Lee et al. (2002)[11]: 10 mL aqueous solutions of $CaCl_2$ and $SrCl_2$ were mixed such that M^{2+} ions were at a concentration of 1 M. To each was added aqueous Na_2CO_3 solution (10 mL, 0.1 M). The solutions were stirred at room temperature for 6 days. Crystals were filtered under reduced pressure and washed with 5 × 1 mL pH-adjusted ultrapure water (pH 9.5, NH_4OH) and 5 × 1 mL ethanol (96 % v/v) and air-dried. Synthetic strontianite was prepared using a similar procedure by mixing 1 M solutions of $SrCl_2$ and Na_2CO_3 at stochiometric ratios. The identity and phase purity of the samples was confirmed by powder X-ray diffraction (**Figure S2**) and the Sr/Ca ratio measured by EDX. EDX was performed using an Oxford Instruments 80 mm^2 X-Max detector with a beam energy of 20 keV, with corresponding scanning electron micrographs using a JEOL JSM-6610LV SEM. Synthetic calcite samples with Sr/Ca ratios of 16 ± 0.5, 30 ± 1 and 45 ± 5 mmol mol^{-1} were prepared as XANES pellets. The spectra were similar, and the shown "calcite" spectrum is an average of the three samples. Pellets of the standards were prepared using cellulose as a binder, and encased in Kapton tape for measurement on the beamline. These were measured for 0.1-1 s per energy depending on concentration. Data was processed using Athena and absolute energies were corrected using the Y k-edge of an yttrium foil as a reference.

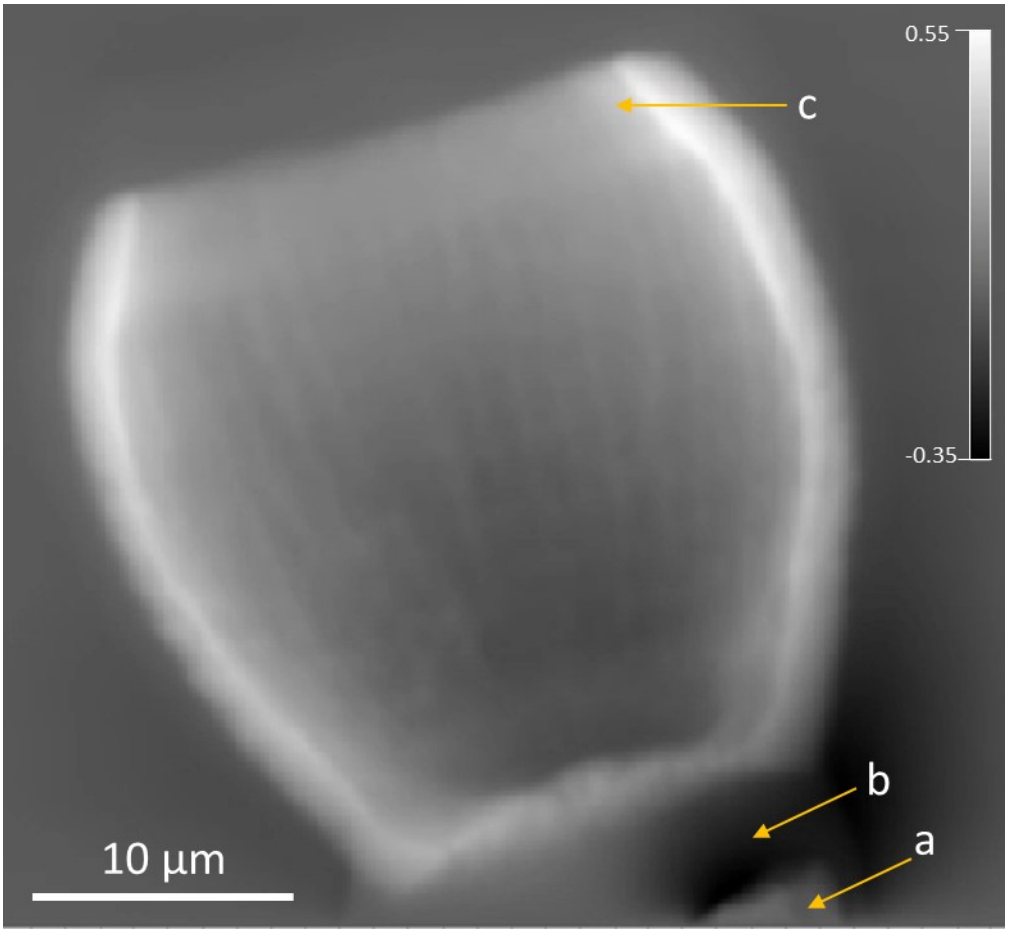

Figure S1. The *S. apsteinii* lopadolith studied by tomography, visualised by integrated differential phase contrast imaging.[4, 12] **a)** The tip of the steel insect pin; **b)** Epoxy resin used as a fixative; **c)** A thicker section near the rim of the lopadolith. Scale in mrad.

Table S1 – Ca and Sr max counts for the XRF maps in Figures 3-5

Figure	Pixel size (nm)	Count time (s) /pixel	Ca max counts	Sr max counts	Ca max cps	Sr max cps
3	60	0.75	12982	5717	17309	7623
4A	100	0.5	2784.05	1656.9	5568	3314
4B	50	1	17642.4	8506	17642.4	8506
4C	50	0.15	1338.34	516.78	8922	3445
5a-d	60	0.05	358	595	7160	11900
5e-h	60	0.05	278	588	5560	11760
5i-l	60	0.05	260	446	5200	8920
5m-p	60	0.05	309	528	6180	10560

Powder X-ray diffraction (PXRD)

PXRD data were collected using a Bruker D8 Advance setup with parallel beam vertically collimating optics using Cu Kα radiation and a Vantec 1-D Bruker detector. Samples were mounted as a thin layer of powder on polished Si plates, cut to a forbidden plane so as not to give any diffraction peaks. A sample of *Scyphosphaera* coccoliths were prepared by drop casting directly onto a Si plate from a suspension in ethanol. Samples were scanned in the range $20° \leq 2\theta \leq 70°$ at intervals of ~0.01° with a count time > 1 s.

Energy Dispersive X-ray Spectroscopy (EDX)

Synthetic calcite samples were drop-cast onto glass cover slips from a suspension in ethanol. SEM samples were sputter coated with 10 nm Pt using a Quorum Q150T ES. Scanning electron micrographs were collected using a JEOL JSM-6610LV instrument. EDS was conducted using an Oxford Instruments 80 mm^2 X-Max detector with a beam energy of 20 keV. An acquisition time of 150 s live time was used with the detector dead time in the range 30 – 50 %. Standardless quantitative EDS analysis was conducted using AZtec (Oxford Instruments).

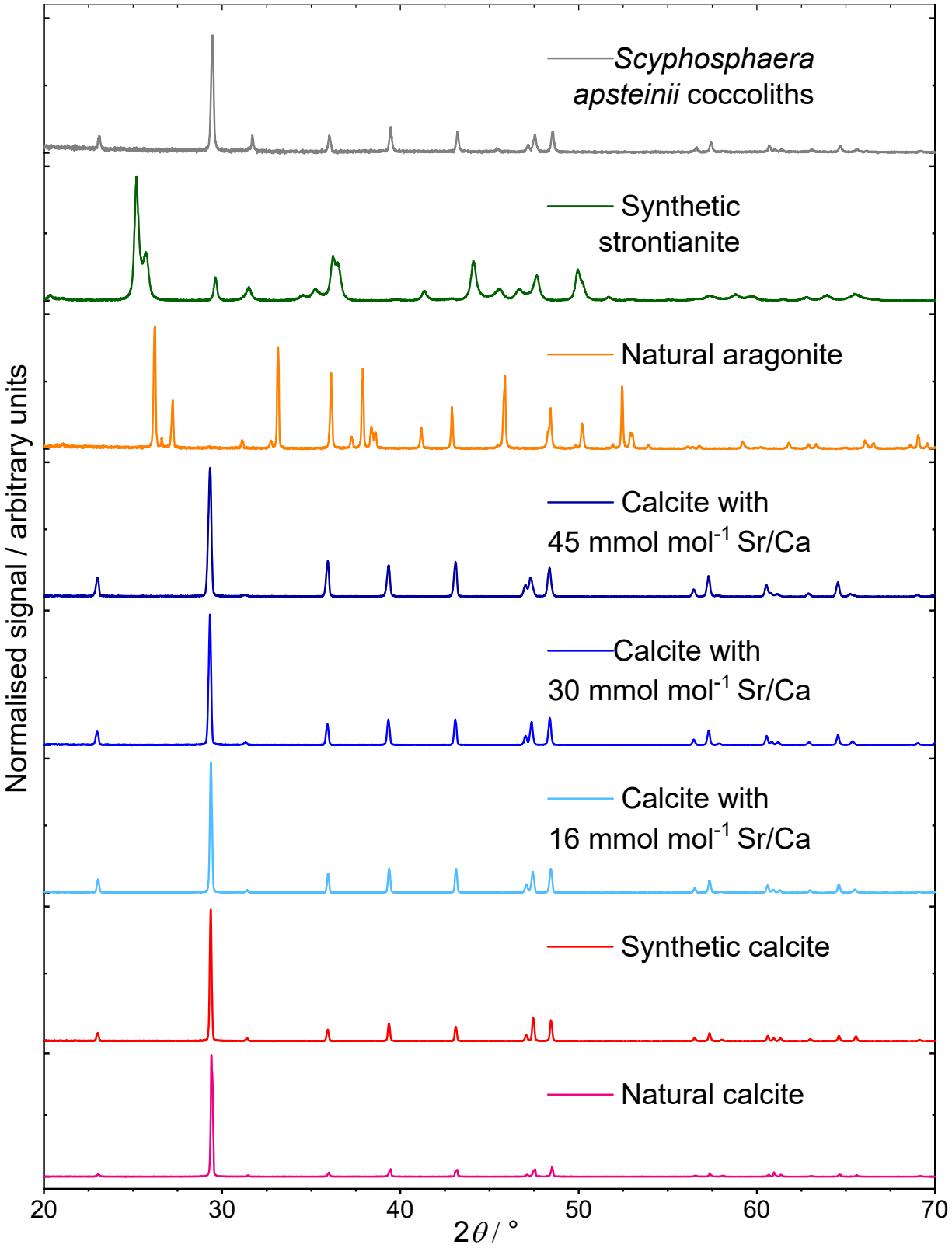

Figure S2. Powder X-ray diffraction patterns from synthetic and natural calcite, aragonite and strontianite samples, and *S. apsteinii* coccoliths. Sr/Ca ratios were determined by EDX.

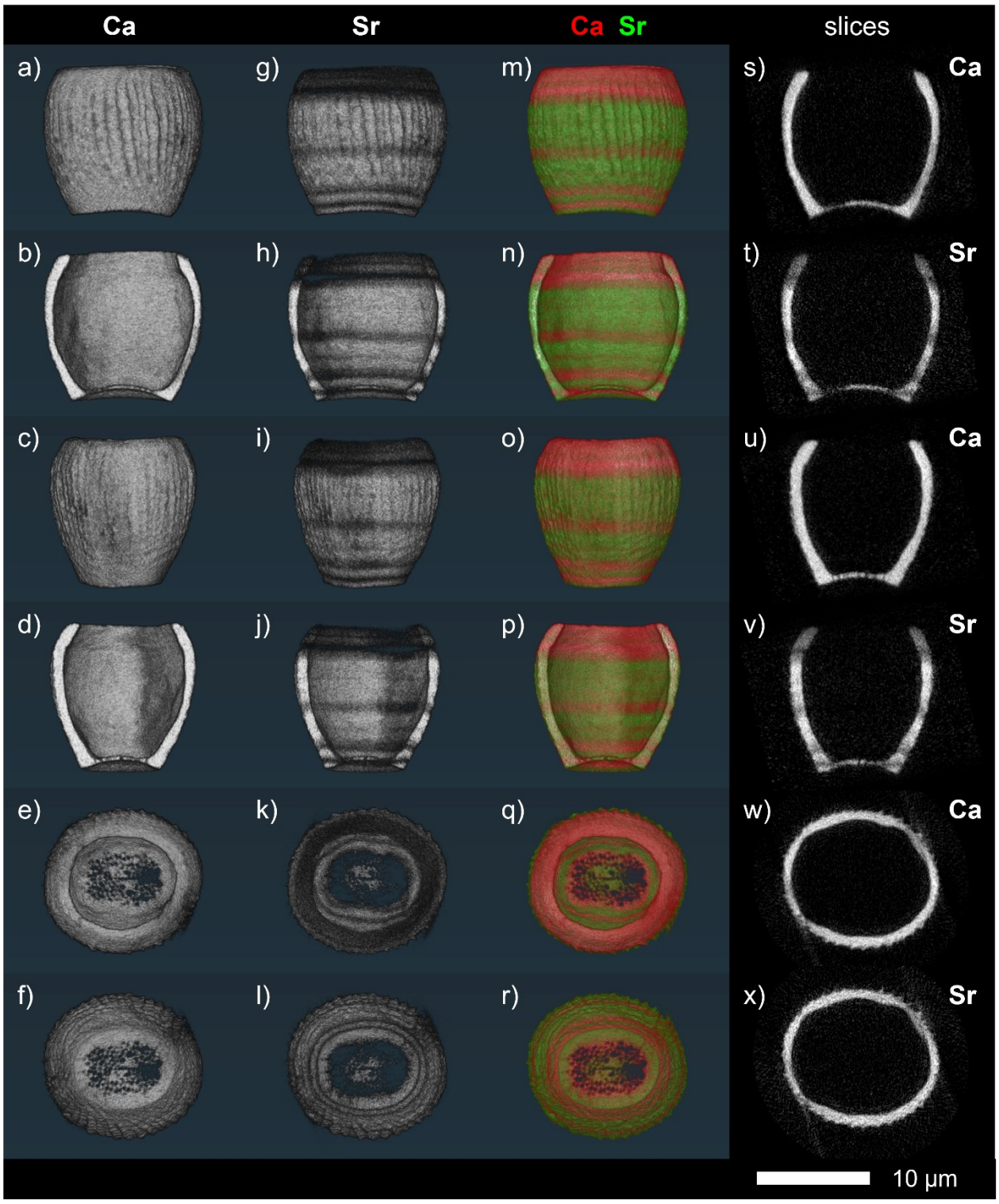

Figure S3. Additional views of the tomographic reconstruction of the *S. apsteinii* lopadolith. **a-f)** Volume rendering of the calcium signal; **g-l)** Volume rendering of the strontium signal; **m-r)** Overlay of the strontium and calcium reconstructions with calcium rendered in red and strontium rendered in green; **s-x)** Slices through the tomogram approximately half way through the lopadolith. Volume renderings **b, h, n** and **d, j, p** are cut along the same plane as slices **s, t** and **u, v** respectively, showing the internal structure of the lopadolith. Volume renderings **e, k, q** present a top-down view and **f, l, r** a base-up view of the lopadolith. The 10 µm scale bar applies to all images.

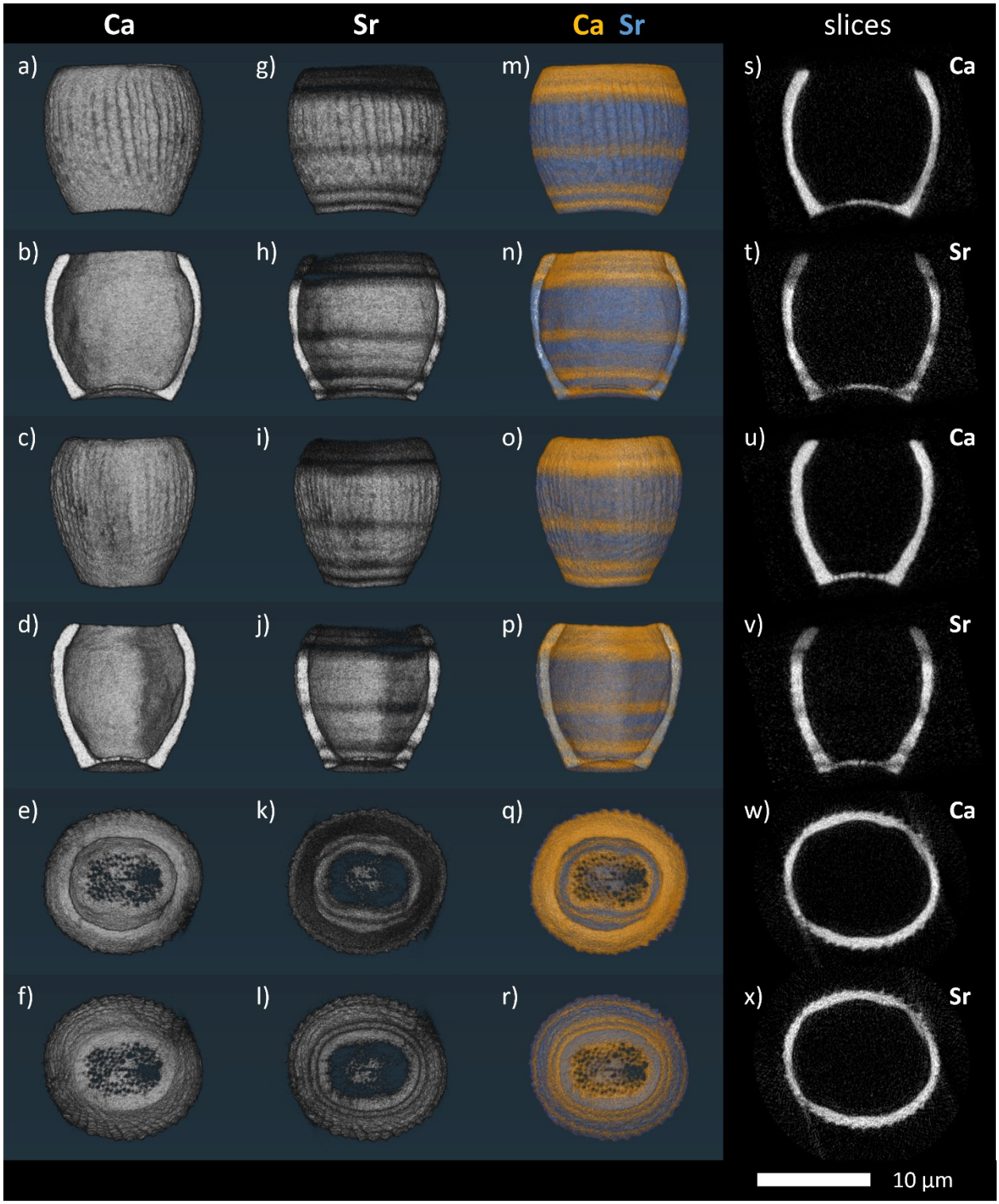

Figure S4. Colourblind-sensitive images from the tomographic reconstruction of the *S. apsteinii* lopadolith **a-f)**, **g-l)**, and **s-x)** as **Figure S3**; **m-r)** Overlay of the strontium and calcium reconstructions with calcium rendered in orange and strontium rendered in blue.

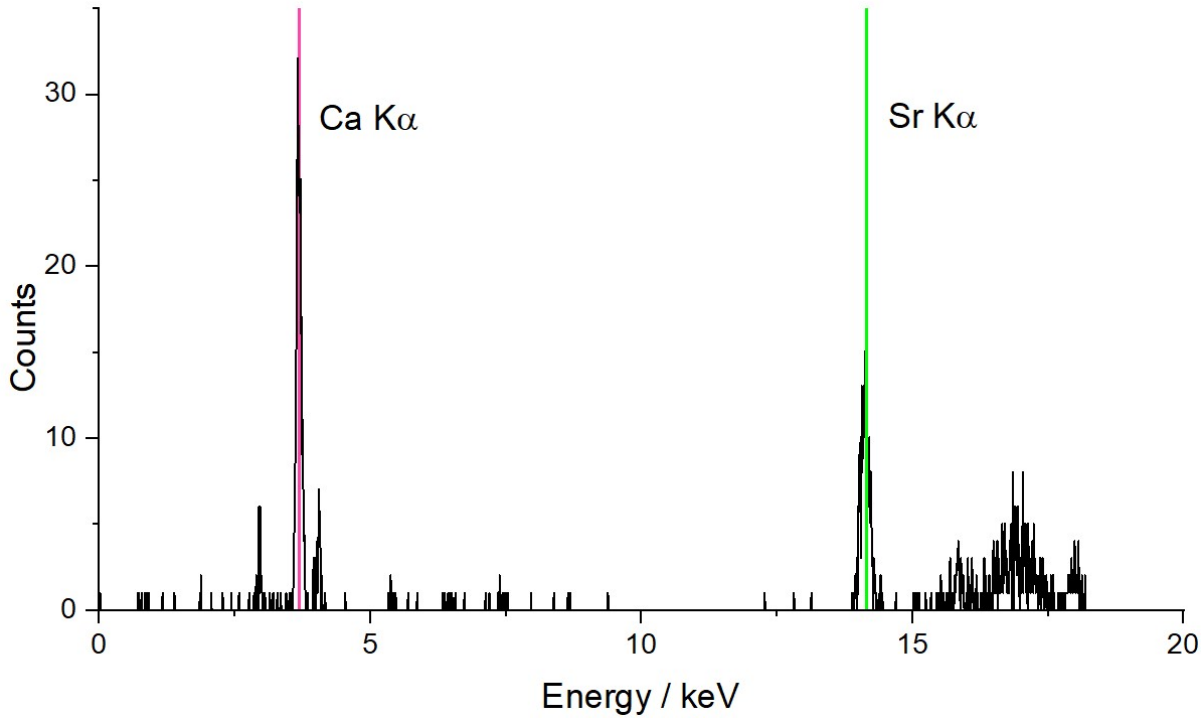

Figure S5. Example raw XRF spectrum from a single pixel (count time 0.02 s/pixel, step size 60 nm) from the tomography data collection. The Ca Kα (red) and Sr Kα X-ray (green) lines are marked.[13]

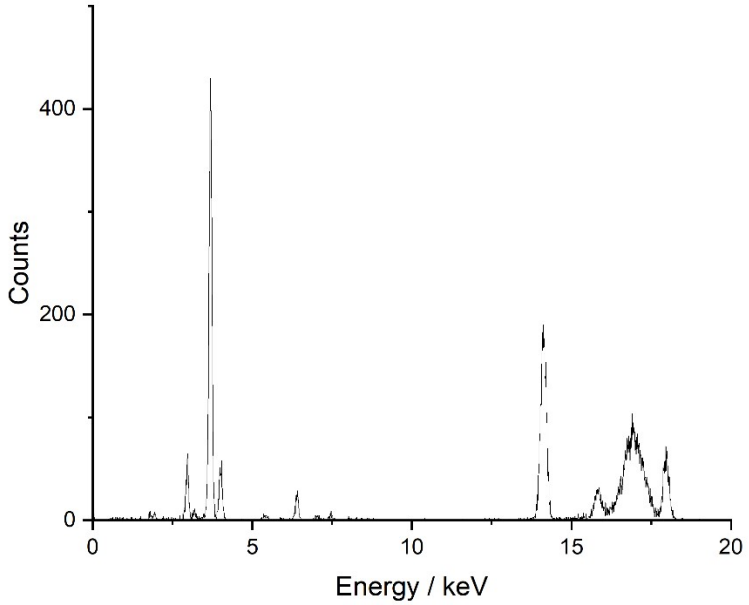

Figure S6. Example raw XRF spectrum from a single pixel (count time 0.75 s/pixel, step size 60 nm) from Figure 3.

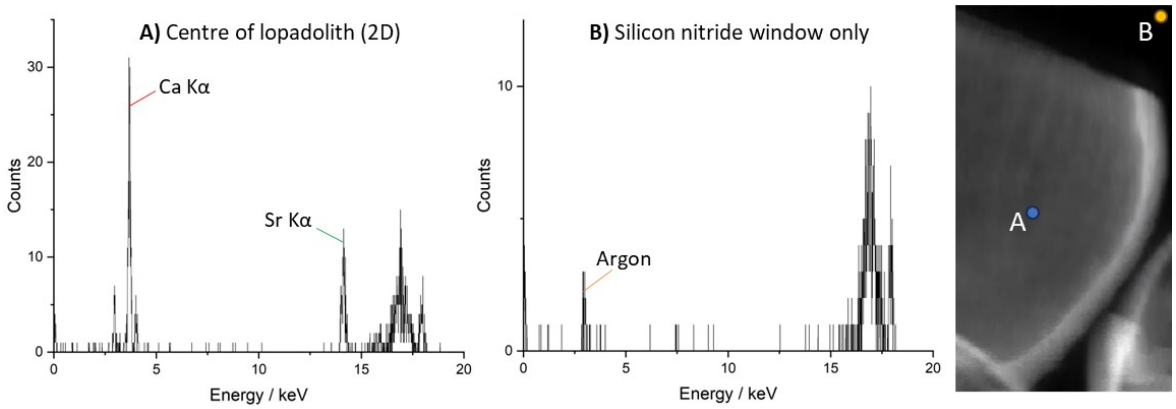

Figure S7. A) Example raw XRF spectrum from a single pixel (count time 0.5 s/pixel, step size 100 nm, blue dot in image) from the centre of a lopadolith that was imaged in 2D on a silicon nitride window, with the Ca Kα (red) and Sr Kα lines marked. **B)** Example raw XRF spectrum from a single pixel of the silicon nitride window (yellow dot, corner of image) behind showing the minimal contribution of the window to the overall spectrum. The peak at 2.958 keV is Argon (yellow) due to the air gap between the sample and the XRF detector. **Image:** Ca signal image of the XRF map used to select pixels for the single pixel spectrum examples. Dots show the position from which the example spectra were taken (blue: A, yellow: B).

Imaging specimens in 2D

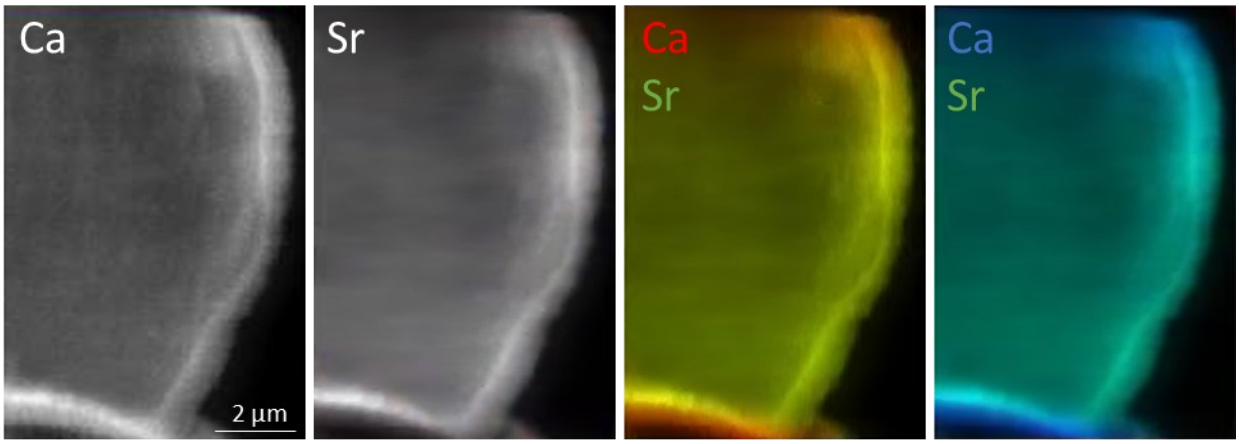

Figure S8. Ca and Sr XRF maps from an additional specimen mapped in 2D with both red/green and blue/green overlaid images. Sr is green in both maps, Ca is either red or blue (50 nm steps, 0.1 s count time at 18 keV). In this specimen, there was a low Sr rim as seen in others, but no specific stripes.

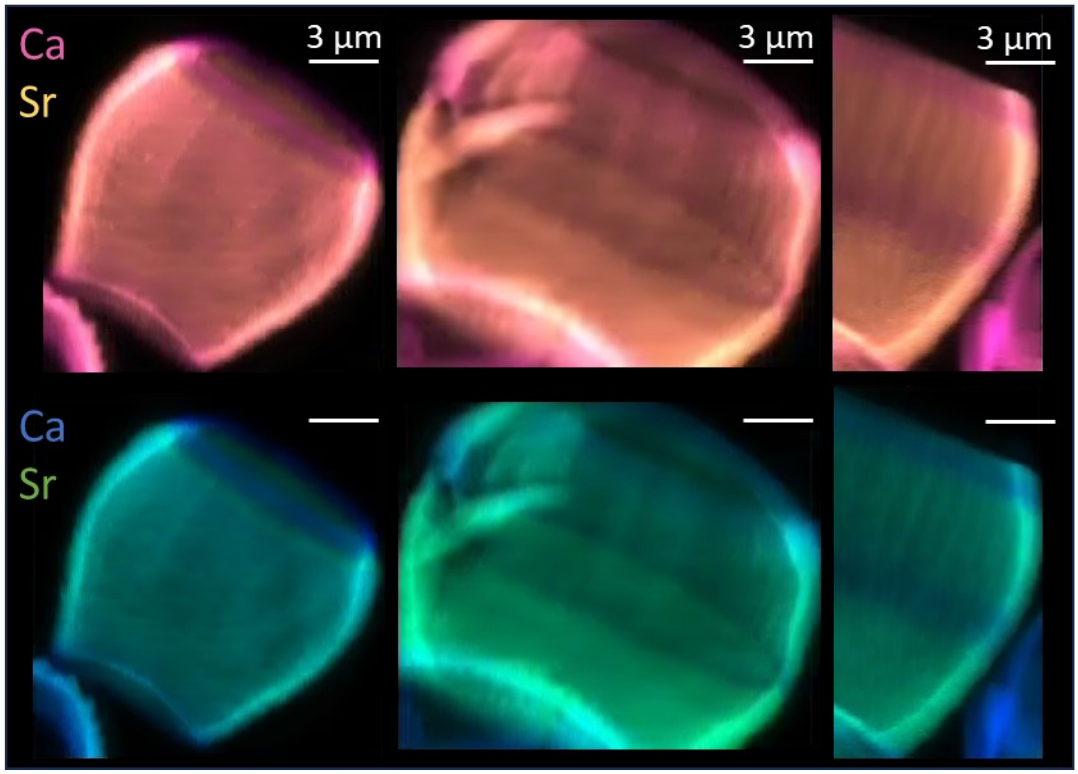

Figure S9. Alternative colour scheme maps for the images shown in Figure 4 (bottom row) of the main text. In the top row, Ca is in magenta and Sr in yellow. In the bottom row, Ca is in blue and Sr in green.

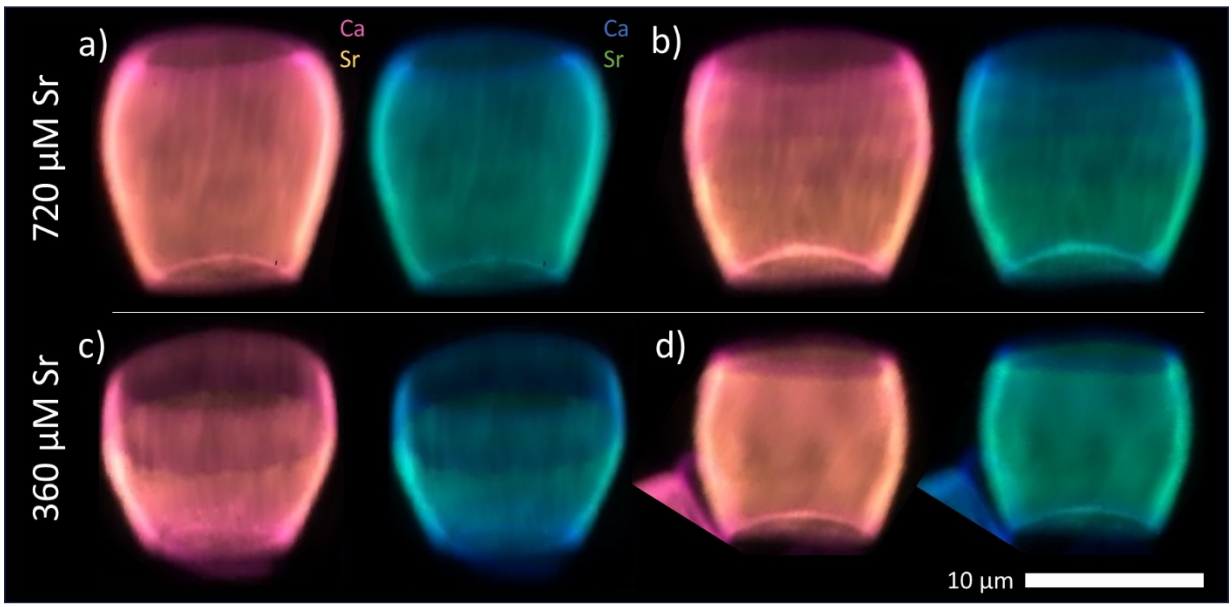

Figure S10. Alternative colour scheme maps for the overlaid Ca and Sr colour maps in Figure 5 of the main text, showing the presence of stripes and the variability between specimens for lopadoliths from cells grown at different concentrations of Sr in the media (left hand side). In these images, the Ca signal is in pink and Sr signal in yellow, or Ca in blue and Sr in green (gradients next to C). Images in a) correspond to image c) in Figure 5. Images in b) correspond to g) in Figure 5. Images in c) correspond to k) in Figure 5 and images in d) correspond to o) in Figure 5 of the main text.

References:

1. R. R. L. Guillard, *Culture of phytoplankton for feeding marine invertebrates*, Plenum Press, New York, NY, USA, 1975.
2. G. Langer, K. Oetjen and T. Brenneis, On culture artefacts in coccolith morphology, *Helgoland Marine Research*, 2013, **67**, 359-369.
3. P. D. Quinn, L. Alianelli, M. Gomez-Gonzalez, D. Mahoney, F. Cacho-Nerin, A. Peach and J. E. Parker, The Hard X-ray Nanoprobe beamline at Diamond Light Source, *J. Synchrotron Rad.*, 2021, **28**, 1006-1013.
4. P. D. Quinn, F. Cacho-Nerin, M. A. Gomez-Gonzalez, J. E. Parker, T. Poon and J. M. Walker, Differential phase contrast for quantitative imaging and spectro-microscopy at a nanoprobe beamline, *Journal of Synchrotron Radiation*, 2023, **30**, 200-207.
5. M. C. Scott, C. Chen, M. Mecklenburg, C. Zhu, R. Xu, P. Ercius, U. Dahmen, B. C. Regan and J. Miao, Electron tomography at 2.4-angstrom resolution, *Nature*, 2012, **483**, 444-447.
6. D. Gursoy, F. D. Carlo, X. Xiao and C. Jacobsen, TomoPy: a framework for the analysis of synchrotron tomographic data, *J. Synchrotron Rad.*, 2014, **21**, 1188-1193.
7. M. Basham, J. Filik, M. T. Wharmby, P. C. Y. Chang, B. E. Kassaby, M. Gerring, J. Aishima, K. Levik, B. C. A. Pulford, I. Sikharulidze, D. Sneddon, M. Webber, S. S. Dhesi, F. Maccherozzi, O. Svensson, S. Brockhauser, G. Naray and A. W. Ashton, Data Analysis WorkbeNch (DAWN), *J. Synchrotron Radiat.*, 2015, **22**, 853-858.
8. W. S. Rasband, ImageJ.*Journal*, 1197-2018.
9. M. Lerotic, R. Mak, S. Wirick, F. Meirer and C. Jacobsen, MANTiS: a program for the analysis of X-ray spectromicroscopy data, *J. Synchrotron Rad.*, 2014, **21**, 1206-1212.
10. J. L. Littlewood, S. Shaw, C. L. Peacock, P. Bots, D. Trivedi and I. T. Burke, Mechanism of Enhanced Strontium Uptake into Calcite via an Amorphous Calcium Carbonate Crystallization Pathway, *Cryst. Growth Des.*, 2017, **17**, 1214-1223.
11. Y. J. Lee, R. J. Reeder, R. W. Wenskus and E. J. Elzinga, Structural relaxation in the MnCO3 - CaCO3 solid solution: a Mn K -edge EXAFS study, *Phys. Chem. Miner.*, 2002, **29**, 585-594.
12. I. Lazić, E. G. Bosch and S. Lazar, Phase contrast STEM for thin samples: Integrated differential phase contrast, *Ultramicroscopy*, 2016, **160**, 265-280.
13. W. T. Elam, B. D. Ravel and J. R. Sieber, A new atomic database for X-ray spectroscopic calculations, *Radiation Physics and Chemistry*, 2002, **63**, 121-128.